УДК 537.6;548.7

Crystal Structure and Magnetism of $Co_{2-x}Ni_xB_2O_5$ Pyroborate

Michael S. Platunov*
Kirensky Institute of Physics, SB RAS,
Akademgorodok, 50/38, Krasnoyarsk, 660036,
Aerospace University,
Krasnoyarsky Rabochy, 31, Krasnoyarsk, 660014,
Russia

Natalya B. Ivanova
Siberian Federal University,
Kirensky, 26, Krasnoyarsk, 660074,
Krasnoyarsk State Agrarian University,
Mira, 90, Krasnoyarsk, 660049,
Russia

Natalya V. Kazak
Leonard N. Bezmaternykh
Alexander D. Vasiliev
Evgeny V. Eremin
Kirensky Institute of Physics, SB RAS,
Akademgorodok, 50/38, Krasnoyarsk, 660036,
Russia

Sergey G. Ovchinnikov
Kirensky Institute of Physics, SB RAS,
Akademgorodok, 50/38, Krasnoyarsk, 660036,
Siberian Federal University,
Kirensky, 26, Krasnoyarsk, 660074,
Aerospace University,
Krasnoyarsky rabochy, 31, Krasnoyarsk, 660014,
Russia

Received 10.01.2011, received in revised form 10.03.2011, accepted 20.04.2011

The high quality single crystals of $Co_2B_2O_5$:Ni were synthesized. The detail study of crystal structure using single-crystal X-ray diffraction was carried out. The monoclinic symmetry was found ($P2_1/c$ space group). The magnetization and magnetic susceptibility measurements have shown antiferromagnetic behavior below $T_N = 47$ K and paramagnetic temperature $\theta = 43$ K. The effective magnetic moment per magnetic ion was 3.49 μ_B, which points out the divalent and high-spin state of Co and Ni ions.

Keywords: transition metal borates, solid state reaction, magnetic susceptibility, magnetic frustration.

Introduction

The pyroborates with general formula MM'B_2O_5, where M and M' are divalent ions Co, Mn, Fe, Mg, Ca, Sr are interesting primarily due to their structural, magnetic and optical properties [1–10]. The crystal structure can be of triclinic or monoclinic symmetry with space group $P\bar{1}(2)$

*platunov@iph.krasn.ru

or $P2_1/c$, respectively. The unit cell contains $Z = 2$ formula units for triclinic structure and $Z = 4$ for monoclinic one. The metal ions are placed inside distorted oxygen octahedra sharing edges and form substructures — *ribbons*. These ribbons are extended along the crystal *b-axis* and contain two distinct crystallographic sites for the metal ions: one in the border columns (1) and another in the central ones (2). In the heterometallic compounds (M $\neq$ M') the metal ions occupy the both sites so that these materials are *intrinsically* disordered. The pyroborate group $(B_2O_5)^{-4}$ formed by two trigonal $(BO_3)^{-3}$ groups is the most strongly bonded. The each of five oxygen ions belongs to the octahedron and the pyroborate group simultaneously. The low-dimensional substructures in the form of *ribbons* and *zigzag walls* are the common feature with another well studied oxyborates, such as warwikites [11] and ludwigites [12].

The magnetic interaction between the neighbor ions within the same ribbon is mainly due to the *super–exchange* mechanism, while the ions belonging to the neighbor ribbons interact through the BO_3 group and, as a consequence, are weakly bonded magnetically. The homometallic pyroborates with M = M' = Fe, Co, Mn show antiferromagnetic behavior with $T_N = 70$ [13], 45 [14] and 24 K [1], respectively. The spin-flop-like transition at 25 kOe was found in $Mn_2B_2O_5$. The magnetic properties of the heterometallic pyroborates $MnMgB_2O_5$ have been studied in detail and random exchange Heisenberg antiferromagnetic chain (REHAC) model was proposed for magnetic behavior description [1]. The magnetic and optical properties study of the powdered $Co_2B_2O_5$ was carried out [14]. The high-spin state of Co^{2+} ions and positive Weiss temperature were found.

In the present work we synthesized the high quality single crystals of Ni — substituted $Co_2B_2O_5$ and investigated the crystal structure and magnetic properties.

1. Experimental Section

The single crystals of $Co_{2-x}Ni_xB_2O_5$ were grown using a flux system $Bi_2Mo_5O_{12}$–Li_2O–B_2O_3–CoO–NiO. The saturation temperature was $T_{sat} \leqslant 980$ °C and the crystallization interval was $\triangle T_{cr} \geqslant 30$ °C. The flux was heated at 1050 °C during 4–6 h and fast cooled down to $T \approx T_{sat}$ — (10–12) °C and then it was slowly cooled with the speed of (4–6) °C/day. The growing process was continued by the three days. The crystals were dark pink in color, circa 3mm long, they had an oblique prism shape and good optical quality. After the reaction the product was subjected to etching in 20 % aqueous solution of nitric acid. The molar ratio of CoO : NiO in the flux was 1 : 0.15, which corresponds to $x = 0.26$.

A room-temperature X-ray diffraction analysis was performed on pink prism-shaped single crystal. The measurements were carried out on a SMART APEX II diffractometer with graphite monochromatic Mo$K\alpha$ radiation ($\lambda = 0.71073$ Å). The structure was solved using the software SHELXS [15] and refined using the software SHELXL–97 [16].

The magnetic properties were investigated using a commercial PPMS 6000 platform (Quantum Design) on powder sample. The temperature dependences of the magnetization and magnetic susceptibility were measured at an applied field of 500 Oe and 2–300 K. The magnetization isotherms were obtained in the field up to 90 kOe and 2–55 K.

2. Results and Discussion

The crystal data for $Co_{2-x}Ni_xB_2O_5$ are summarized in Table 1. The compound crystallizes in a monoclinic structure ($P2_1/c$) while $Co_2B_2O_5$ has a triclinic crystal system [14,17]. The lattice parameters are well agreed with those for $Co_2B_2O_5$ except for b-parameter, which is twofold.

The Table 2 shows the atomic coordinates and anisotropic displacement parameters. The metal ions (Co, Ni) and B have two sites and O atoms have five sites. These sites are at general

$4e$ Wyckoff position. The Table 3 lists the bond lengths, bond angles, bond valence sums (BVS), distortion indices and electric field gradient (EFG) values for $Co_{2-x}Ni_xB_2O_5$.

Table 1. Crystal data and structure refinement

Empirical formula	$Co_4Ni_4B_8O_{20}$
Wavelength	0.71073 Å
Crystal size	0.24×0.06×0.12 mm^3
Temperature	298 K
Crystal system	Monoclinic
Space group	$P2_1/c$
Unit cell parameters	
a, Å	9.2330(22)
b, Å	3.1579(8)
c, Å	12.3593(29)
α	90.000°
β	104.183(3)°
γ	90.000°
V, Å^3	349.4(3)
Z	4
Density (calculated)	4.168 g/cm^3
2θ range (deg)	5–90
Absorption correction	Gaussian
Refinement method	Full-matrix least squares on F^2

Table 2. Atomic coordinates (×10^4) and anisotropic displacement parameters (Å^2 × 10^4) for $Co_{2-x}Ni_xB_2O_5$

Atom	x	y	z	U_{11}	U_{22}	U_{33}	U_{12}	U_{13}	U_{23}
Ni(1)	3569	2052	6049	97.4	110.3	105.9	-10.8	31.7	-9.6
Co(1)	3569	2052	6049	97.4	110.3	105.9	-10.8	31.7	-9.6
Ni(2)	1025	7159	6870	77.4	86.9	95.7	5.2	30.1	4.1
Co(2)	1025	7159	6870	77.4	86.9	95.7	5.2	30.1	4.1
O(1)	2589	2302	7377	33.1	110.6	71.3	18.2	47.9	11.6
O(2)	-536	2198	6528	38.2	109.4	92	4.5	61.6	-6.8
O(3)	4963	-3052	6374	74.3	119.2	113.2	3.2	54.4	18.3
O(4)	1801	-2773	5467	70.9	132.3	62.8	-22.3	47.5	-6.6
O(5)	2984	701	4292	57.6	117.9	77.1	-24.8	9.5	-1.5
B(1)	-1682	1525	5609	85.1	64.4	106.7	6.2	12	-10.3
B(2)	3553	2766	8405	100.3	48.5	98.4	-22.1	81.9	-28.6

Fig. 1 shows the coordination environments around metal and boron atoms. The composite ion B_2O_5 is formed by two $B1O_3$ and $B2O_3$ triangles linked by sharing O5 atom. The metal Co/Ni atoms are surrounding by the distorted oxygen octahedra. The structure of $Co_{2-x}Ni_xB_2O_5$ projected to the *ac*-plane is shown in Fig. 2, a. Four $(Co,Ni)O_6$ octahedra, linked by edge-sharing, are aligned in the chain of the (Co,Ni)1–(Co,Ni)2–(Co,Ni)2–(Co,Ni)1 and form the $(Co,Ni)_4O_{18}$ units. These units are extended along b-axis and form a *ribbon* substructure. The Fig. 2, b represents the ribbon substructure along b-axis. The each ribbon represents almost hexagonal lattice of Co/Ni ions. The mean closest interatomic M–M distance is 3.1686(1) Å.

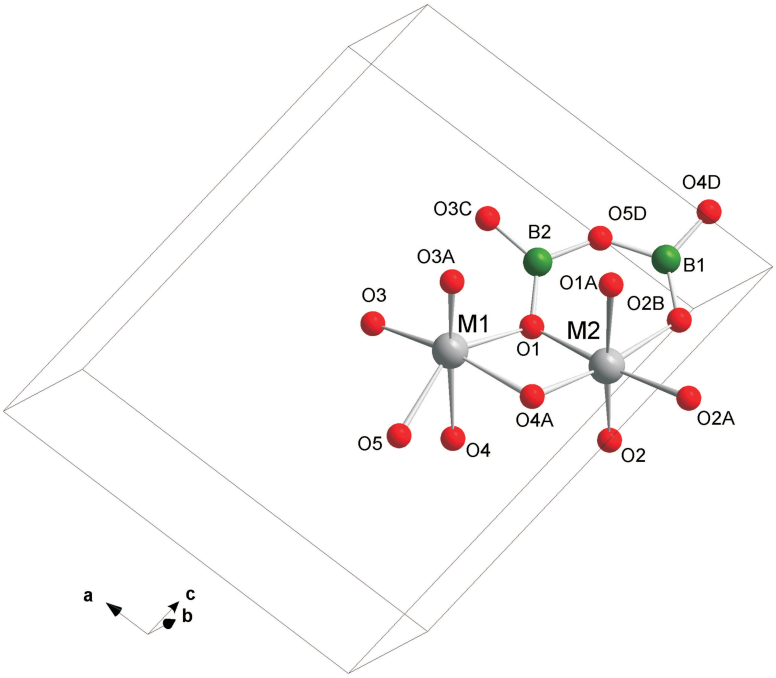

Fig. 1. Metal and boron coordination environment in $Co_{2-x}Ni_xB_2O_5$. The symmetry labels correspond to those defined in Table 3

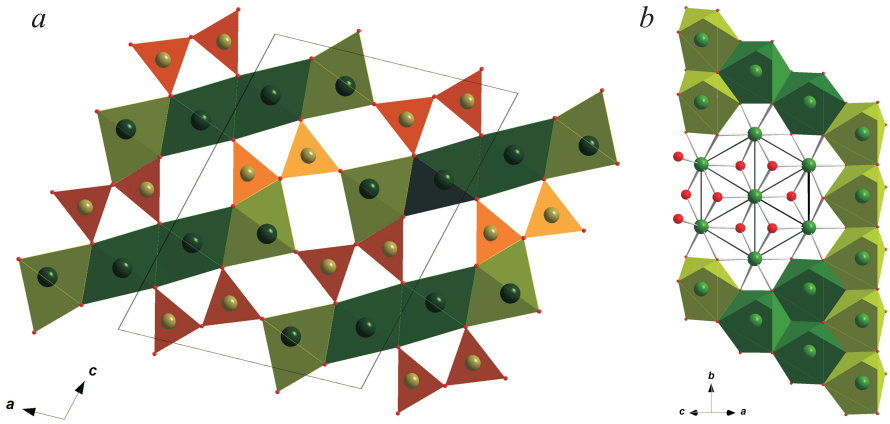

Fig. 2. a) Crystal structure of $Co_{2-x}Ni_xB_2O_5$ viewed in the *ac*-plane. b) The ribbon plot showing the hexagonal arrangement of metal ions. The M1 and M2 sites are marked by light and dark octahedra, respectively

We have estimated the valence state of metal (M1, M2) and boron ions by means of the bond valence sum calculation

$$Z = \sum_{i=1} s_{ij}, \quad s_{ij} = \exp\left[\frac{(R_0 - r_{ij})}{b}\right]. \tag{1}$$

Here s_{ij} — the bond valence between i and j ions, R_0 — the bond valence parameter (BVP)

dependent on the nature of ions forming the ij-pair, b — the constant value 0.37 Å, r_{ij} is the distance between i and j atoms [6, 18, 19]. The BVP values for Co^{2+}, Ni^{2+} and B^{3+} are 1.692, 1.654, and 1.371 Å, respectively. The calculations of bond valence sum for B at the triangular coordination and M at the octahedral one were shown that boron and cobalt/nikel are trivalent and divalent, respectively (see Table 3).

The interatomic distances inside BO_3 group appeared to be very short. When calculated from the above parameters they are found to be: mean B–O bond lengths are 1.3850(3) and 1.3785(6) for B1 and B2, respectively. The closeness of mean B–O–B bond angle to 120° corresponds to with the trigonal planar geometry [9]. The Co/Ni-O bond lengths range from 1.9891(4) to 2.2973(4) for the atoms at the octahedral site 1 and from 2.0319(4) to 2.1616(4) for ones at the octahedral site 2. From the interatomic distances given above it is seen that the connection forces within the B_2O_5 group undoubtedly must be much stronger than the other bonds. There exist a large dispersion in the bond angles of both octahedra. The O–(Co/Ni)–O bond angles range from 63.49° to 110.38° for Co1/Ni1 and from 82.37° to 101.75° for Co2/Ni2. The distortion index of $(Co1/Ni1)O_6$ octahedron is three times larger than that of $(Co2/Ni2)O_6$.

The distortions degree of oxygen octahedra M_1O_6 and M_2O_6 also can be estimated according the value of electric field gradient (EFG). The lattice sums calculations made for the oxides with the spinel structure have shown that oxygen anions, belonging to the closest coordination octahedra, sufficiently screen the contribution from the next-nearest coordination spheres [20]. Therefore, we limited our calculation by the contribution from the first coordination sphere. In this case the mane component V_{ZZ} of the EFG tensor may be calculated as

$$V_{ZZ} = \sum 2e \frac{3\cos^2\theta - 1}{r^3}, \tag{2}$$

where e — elementary charge, θ — the angle between the main axis (z) of EFG tensor and the adjacent oxygen ion direction, r — the metal — oxygen distance. The results are given in the Table 3. One can see that site 2 has more symmetric oxygen surrounding, while the M_1O_6 octahedra situated at the ribbons edges are exceedingly distorted. This conclusion well agree with those reported for the other isotypic pyroborates such as $CoMnB_2O_5$, $M_{1.5}Zn_{0.5}B_2O_5$ (M = Co, Ni).

The intra-ribbon distances Co1/Ni1–Co2/Ni2 and Co2/Ni2–Co2/Ni2 are 3.1786–3.2121 and 3.1526–3.1579 Å, respectively. The closest inter-ribbons metal distances Co1/Ni1–Co1/Ni1 and Co2/Ni2–Co2/Ni2 are 4.2069(7) Åand 4.8872(9) Å, respectively. The closest distances Co1/Ni1–Co1/Ni1 for coplanar ribbons and for adjacent ones are 4.5316(7) and 4.2069(7) Å, respectively.

The temperature dependencies of the *ac*-susceptibility real part for the different frequencies are shown in Fig. 3. The sharp peak near 47 K and small divergence at low temperatures are visible. According to the M(T) form this magnetic transition can be identified as an antiferromagnetic one. It is in agreement with the results of T. Kawano et al [14]. There is no frequency dependence of T_N.

Fig. 4 shows the temperature dependence of the inverse *dc*-susceptibility measured in a magnetic field 500 Oe. The high-temperature susceptibility is well fitted by Curie-Weiss equation $\chi = C/(T - \theta_{CW})$, with $\theta_{CW} = 43$ K indicating on the predominance of ferromagnetic interactions in the system. The FM interaction was found also for the parent $Co_2B_2O_5$ but it is much weaker ($\theta_{CW} = 7.7$ K) comparing $Co_{2-x}Ni_xB_2O_5$. The Curie constant $C = 1.53$ emu·K·mol^{-1}·Oe^{-1} per magnetic ion. The effective magnetic moment per magnetic ion $\mu_{eff} = 3.49\ \mu_B$. The μ_{eff} value is less than one for the parent compound and points out the divalent and high-spin state of the Co and Ni ions. The substitution of the part of Co^{2+} ($S = 3/2$) ions by Ni^{2+} ($S = 1$) ones should give rise to the magnetic moment decreasing, as it is observed. All the magnetization isotherms obtained at $T = 2 - 40$ K are linear. Two of them are shown in Fig. 5. The magnetic susceptibility in the antiferromagnetic state $\chi_{AF} = 2.01 \cdot 10_{-5}\mu_B$/f.u./Oe ($T = 2$ K). The curves above the magnetic transition are typical for paramagnetic behavior.

Table 3. Bond lengths (Å), angles (deg), bond valence sum (BVS), distortion indices and the main component V_{ZZ} of the electric field gradient for $Co_{2-x}Ni_xB_2O_5$

Cobalt (nikel) coordination			
Co1/Ni1 – O1	2.0601(4)	Co2/Ni2 – O1	2.0950(4)
Co1/Ni1 – O3	2.0407(4)	Co2/Ni2 – O1A	2.1616(4)
Co1/Ni1 – O3A	1.9891(4)	Co2/Ni2 – O2	2.1003(4)
Co1/Ni1 – O4	2.2199(4)	Co2/Ni2 – O2A	2.1185(4)
Co1/Ni1 – O4A	2.2973(4)	Co2/Ni2 – O2B	2.1360(5)
Co1/Ni1 – O5	2.1480(5)	Co2/Ni2 – O4A	2.0319(4)
O4A – Co1/Ni1 – O5	80.898(4)	O2A – Co2/Ni2 – O4A	100.731(5)
O1 – Co1/Ni1 – O4A	78.755(4)	O2A – Co2/Ni2 – O2B	83.876(4)
O1 – Co1/Ni1 – O3	104.633(6)	O1 – Co2/Ni2 – O2B	90.801(5)
O3 – Co1/Ni1 – O5	91.835(5)	O1 – Co2/Ni2 – O4A	84.328(5)
O4 – Co1/Ni1 – O5	63.493(4)	O2 – Co2/Ni2 – O4A	101.751(5)
O1 – Co1/Ni1 – O4	81.527(4)	O2A – Co2/Ni2 – O2	96.926(4)
O4A – Co1/Ni1 – O4	88.688(4)	O2B – Co2/Ni2 – O2	84.314(4)
O3 – Co1/Ni1 – O4	84.271(5)	O1 – Co2/Ni2 – O2	84.420(5)
O3A – Co1/Ni1 – O5	110.379(5)	O1A – Co2/Ni2 – O4A	83.616(4)
O3A – Co1/Ni1 – O4A	83.427(5)	O1A – Co2/Ni2 – O2A	82.370(5)
O1 – Co1/Ni1 – O3A	101.444(6)	O1A – Co2/Ni2 – O2B	90.301(5)
O3 – Co1/Ni1 – O3A	103.181(4)	O1 – Co2/Ni2 – O1A	95.772(4)
O3A – Co1/Ni1 – O4	170.818(6)	O1 – Co2/Ni2 – O2A	174.340(6)
O1 – Co1/Ni1 – O5	139.662(6)	O2B – Co2/Ni2 – O4A	171.772(6)
O3 – Co1/Ni1 – O4A	171.600(5)	O1A – Co2/Ni2 – O2	174.615(5)
Boron coordination			
B1 – O2B	1.3656(2)	B2 – O3C	1.3544(3)
B1 – O4D	1.3665(3)	B2 – O1	1.3694(2)
B1 – O5D	1.4230(3)	B2 – O5D	1.4119(2)
O2B – B1 – O4D	128.686(8)°	O1 – B2 – O5D	118.472(8)°
O2B – B1 – O5D	120.313(9)°	O1 – B2 – O3C	124.175(10)°
O5D – B1 – O4D	110.996(8)°	O3C – B2 – O5D	117.33(1)°
B1 – B2	2.6278(4)	B1 – O5 – B2	135.922(9)°
	Bond valence sum		
Co1/Ni1	1.93/1.75		
Co2/Ni2	1.96/1.77		
B1	2.89		
B2	2.95		
	Distortion index	V_{ZZ}, $e/Å^3$	
$(Co1/Ni1)O_6$	0.045	0.167	
$(Co2/Ni2)O_6$	0.015	-0.024	

Symmetry transformations used to generate equivalent atoms: A: x, 1+y, z; B: –x, 0.5+y, 1.5–z; C: 1–x, 0.5+y, 1.5–z; D: x, 0.5–y, 0.5+z.

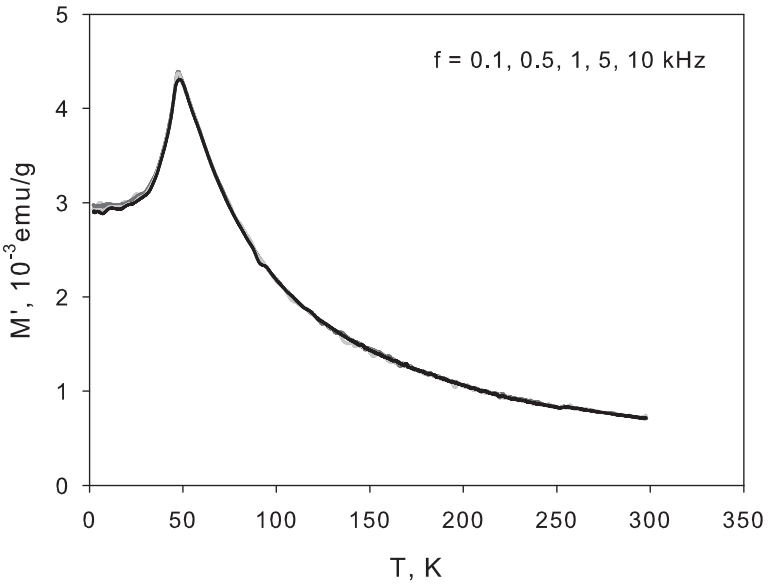

Fig. 3. The real part of the *ac*-magnetization for different frequencies. The magnetic field amplitude is 10 Oe

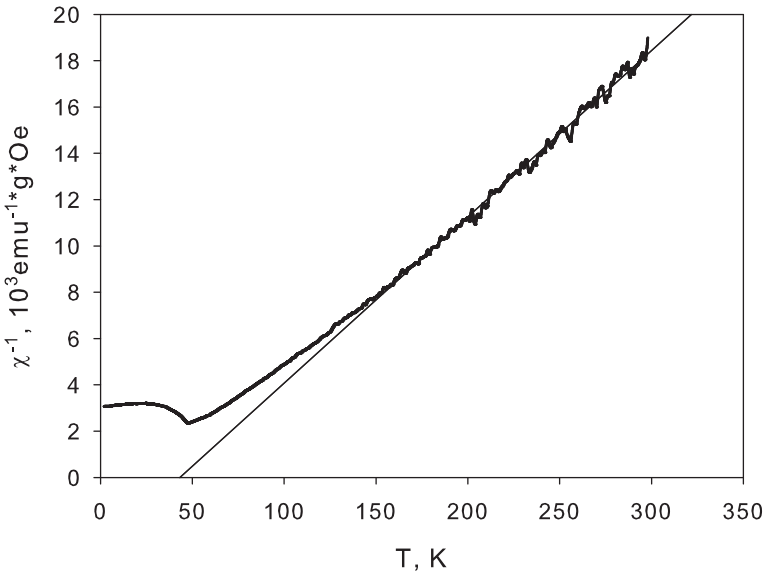

Fig. 4. The temperature dependence of inverse *dc*-susceptibility measured in the field H=500 Oe. The straight line is guided by the eye

The intra-ribbon M1–M2 and M2–M2 distances are close to 3 Å, therefore the direct exchange in $Co_{2-x}Ni_xB_2O_5$ is hardly possible. This situation unlikely is in contrast to the case of ludwigites, where the interatomic distances are close to the same [12]. So only the superexchange interactions are possible. The closest inter-ribbons M1—M1 and M2–M2 distances exceed 4.2 Å.

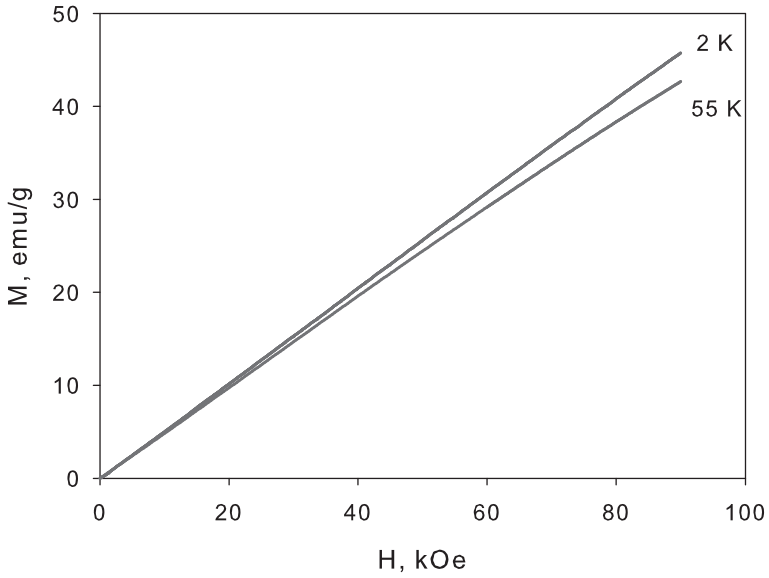

Fig. 5. Magnetization isotherms

The deviation from the Curie-Weiss law reveals below 150 K, that is much higher the magnetic transition point T_N (Fig. 4). This indicates the strong ferromagnetic correlations in the system. The fact of large positive value of $|\theta_{CW}| \approx T_N$ indicates that FM and AFM interactions are congruous in $Co_{2-x}Ni_xB_2O_5$.

The behavior of $Co_{2-x}Ni_xB_2O_5$ is typical for antiferromagnet but not for the frustrated system as it can be expected from an almost hexagonal network of the Co(Ni)1 and Co(Ni)2 ions in the ribbons (Fig. 2, b). Nevertheless in the case of hexagonal structure the AFM interaction between the magnetic ions belonging to the one ribbon presently produce the frustrated magnetic bonds. The spin ordering questing was brought up in the work [3]. Using the maximum-entropy method for the calculation electron density distribution in the (100) plane the authors proposed a model of spin configurations in $Mn_2B_2O_5$ below T_N. According to this model, the magnetic interaction inside the coplanar ribbons is FM, and the AFM interaction develops between the adjacent ribbons. This model suits for the description of $Co_{2-x}Ni_xB_2O_5$ magnetic behavior: one can suppose that $|\theta_{CW}|$ value is determined by FM intra-ribbons superexchange interaction and T_N value is due to AFM inter-ribbons superexchange interaction through $(BO_3)^{3-}$ anion.

We estimated the intra-ribbons exchange integral by means of the mean field (MF) prediction $|\theta_{CW}| = \dfrac{2zJ\overline{S}(\overline{S}+1)}{3k}$, where $\overline{S}$ is an average magnetic moment per magnetic ion determined as $\overline{S} = ((2\text{-}x)\cdot 3/2 + x\cdot 1)/2$, z denotes the number of nearest-neighboured Co^{2+} and Ni^{2+} spins. With $z = 2$ we obtain $J/k_B \sim 9.23$ K.

Conclusion

The single crystals of $Co_{2-x}Ni_xB_2O_5$ pyroborate were prepared using a *flux method*. The crystal structure study has shown the monoclinic modification whereas the parent $Co_2B_2O_5$ has the triclinic crystal structure. The magnetization and magnetic susceptibility study have shown the antiferromagnetic ordering below $T_N = 47$ K. The positive Curie-Weiss temperature θ just as in $Co_2B_2O_5$ indicates the predomination of the ferromagnetic interaction between the magnetic

ions, which is stronger in the Ni-substituted sample. The effective magnetic moment (μ_{eff} = 3.49 μ_B) indicates that the magnetic ions Co(Ni) are divalent and are in a high-spin state. The substitution of the part of Co^{2+} ($S = 3/2$) ions by Ni^{2+} ($S = 1$) leads to decrease in average magnetic moment per formula unit.

This study was supported by the Russian Foundation for Basic Research (project no. 09-02-00171-a), the Federal Agency for Science and Innovation (Rosnauka) (project no. MK-5632.2010.2), the Physical Division of the Russian Academy of Science, the program "Strongly Correlated Electrons", project 2.3.1.

References

[1] J.C.Fernandes, F.S.Sarrat, R.B.Guimaraes, R.S.Freitas, M.A.Continentino, A.C.Doriguetto, Y.P.Mascarenhas, J.Ellena, E.E.Castellano, J-L.Tholence, J.Dumas, L.Chivelder, Structure and magnetism of $MnMgB_2O_5$ and $Mn_2B_2O_5$, *Phys. Rev. B*, **67**(2003), 104413.

[2] S.C.Neumair, H.Huppertz, Synthesis and Crystal Structure of the Iron Borate $Fe_2B_2O_5$, *Z. Naturforsch.*, **64b**(2009), 491-498.

[3] F.S.Sarrat, R.B.Guimaraes, M.A.Continentino, J.C.Fernandes, A.C.Doriguetto, J.Ellena, Electron density distribution in the pyroborate $Mn_2B_2O_5$ studied by the maximum-entropy method, *Phys. Rev. B*, **71**(2009), 224413.

[4] G.C.Guo, W.D.Cheng, J.T.Chen, J.S.Huang, Q.E.Zhang, Monoclinic $Mg_2B_2O_5$, *Acta Cryst. C*, **51**(1995), 351.

[5] W.D.Cheng, H.Zhang, F.K.Zheng, J.T.Chen, Q.E.Zhang, R.Pandey, Electronic Structures and Linear Optics of $A_2B_2O_5$ (A = Mg, Ca, Sr) Pyroborates, *Chem. Mater.*, **12**(2000), 3591.

[6] T.Mimani, Samrat Grosh, Combustion synthesis of cobalt pigments: Blue and pink, *Current Science*, **78**(2000), no. 7, 892.

[7] A.F.Qasrawi, T.S.Kayed, A.Mergen, M.Guru, Synthesis and Characterisation of $Mg_2B_2O_5$, *Mater. Res. Bull.*, **40**(2005), 583.

[8] A.Obut, Thermal syntheses of magnesium borate compounds from high-energy milled MgO–B_2O_3 and MgO–$B(OH)_3$ mixtures, *Journal of Alloys and Compounds*, **457**(2008), 86.

[9] S.V.Berger, The Crystal Structure of Cobaltpyroborate, *Acta Chem. Scand.*, **4**(1950), 1054.

[10] Y.Takeuchi, The crystal structure of magnesium pyroborate, *Acta Cryst.*, **5**(1952), 574.

[11] M.A.Continentino, A.M.Pedreira, R.B.Guimaraes, M.Mir, J.C.Fernandes, R.S.Freitas, L.Ghivelder, Specific heat and magnetization studies of Fe_2OBO_3, Mn_2OBO_3, and $MgScOBO_3$, *Phys. Rev. B*, **64**(2001), 014406.

[12] N.V.Kazak, N.B.Ivanova, O.A.Bayukov, S.G.Ovchinnikov, A.D.Vasiliev, V.V.Rudenko, J.Bartolomé, A.Arauzo, Yu.V.Knyazev, The superexchange interactions in mixed Co–Fe ludwigite, *J.M.M.M.*, **323**(2011), 521.

[13] T.Kawano, H.Morito, H.Yawade, T.Onuma, Sh.F.Chichibu, H.Yawane, Synthesis, crystal structure and characterization of iron pyroborate ($Fe_2B_2O_5$) single crystals, *J. Solid State Chem.*, **182**(2009), 2004.

[14] T.Kawano, H.Morito, H.Yawane, Synthesis and characterization of manganese and cobalt pyroborates: $M_2B_2O_5$ (M = Mn, Co) , *J. Solid State Sciences*, **12**(2010), 1419.

[15] G.M.Sheldrick, Phase Annealing in Shelx-90: Direct Methods for Lager Structures, *Acta Cryst. A*, **46**(1990), 467–473.

[16] G.M.Sheldrick, Shelxl-97: a computer program for refinement of crystal structures, Acta Cryst. A, University of Göttingen, Germany (1997).

[17] J.L.C.Rowsell, N.J.Taylor, L.F.Nazar, Crystallographic investigation of the Co–B–O system, *J. Solid State Chem.*, **174**(2003), 189.

[18] R.M.Wood, G.J.Palenik, Bond Valence Sums in Coordination Chemistry. A Simple Method for Calculating the Oxidation State of Cobalt in Complexes Containing Only Co–O Bonds, *Inorg. Chem.*, **37**(1998), 4149.

[19] N.E.Brese, M.O'Keeffe, Bond-valence parameters for solids, *Acta Cryst. B*, **47**(1991), 192.

[20] G.A.Petrakovskii, L.N.Bezmaternykh, D.A.Velikanov, A.M.Vorotynov, O.A.Bayukov, M.Schneider, Magnetic Properties of Single Crystals of Ludwigites Cu_2MBO_5 (M = Fe^{3+}, Ga^{3+}), *Physics of Solid State*, **51**(2009), 2077.

Кристаллическая структура и магнетизм пиробората $Co_{2-x}Ni_xB_2O_5$

Михаил С. Платунов
Наталья Б. Иванова
Наталья В. Казак
Леонард Н. Безматерных
Александр Д. Васильев
Евгений В. Еремин
Сергей Г. Овчинников

Синтезированы высококачественные монокристаллы $Co_2B_2O_5$:Ni. Проведено детальное исследование кристаллической структуры с использованием монокристаллического рентгеновского дифрактометра. Обнаружена моноклинная симметрия (пространственная группа $P2_1/c$ [14]). Измерения намагниченности и магнитной восприимчивости выявили антиферромагнитный переход при $T_N = 47$ K и парамагнитную температуру $\theta = 43$ K. Эффективный магнитный момент, приходящийся на магнитный ион, найден равным 3.49 μ_B, что указывает на двухвалентное и высокоспиновое состояния ионов Co и Ni.

Ключевые слова: бораты переходных металлов, твердотельная реакция, магнитная восприимчивость, магнитная фрустрация.